ACS APPLIED MATERIALS & INTERFACES

Research Article

www.acsami.org

Modification of Graphene/SiO_2 Interface by UV-Irradiation: Effect on Electrical Characteristics

Gaku Imamura* and Koichiro Saiki

Department of Complexity Science and Engineering, The University of Tokyo, Kashiwanoha 5-1-5, Kashiwa, Chiba 277-8561, Japan

Supporting Information

ABSTRACT: Graphene is a promising material for next-generation electronic devices. The effect of UV-irradiation on the graphene devices, however, has not been fully explored yet. Here we investigate the UV-induced change of the field effect transistor (FET) characteristics of graphene/SiO_2. UV-irradiation in a vacuum gives rise to the decrease in carrier mobility and a hysteresis in the transfer characteristics. Annealing at 160 °C in a vacuum eliminates the hysteresis, recovers the mobility partially, and moves the charge neutrality point to the negative direction. Corresponding Raman spectra indicated that UV-irradiation induced D band relating with defects and the annealing at 160 °C in a vacuum removed the D band. We propose a phenomenological model for the UV-irradiated graphene, in which photochemical reaction produces dangling bonds and the weak sp^3-like bonds at the graphene/SiO_2 interface, and the annealing restores the intrinsic graphene/SiO_2 interface by removal of such bonds. Our results shed light to the nature of defect formation by UV-light, which is important for the practical performance of graphene based electronics.

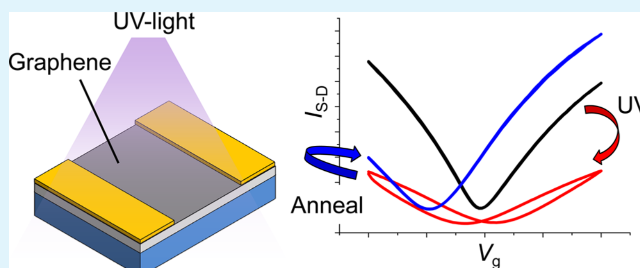

KEYWORDS: *graphene, defect formation, field effect transistors, carrier doping, photochemical reactions, Raman spectroscopy*

INTRODUCTION

Graphene, a one atom thick sheet composed of sp^2 carbon atoms, has been studied intensively for future electronics, optics, and energy technology.[1,2] Due to its high optical transparency and high conductivity, graphene is a promising material for transparent electrodes, which can be used for photovoltaic cells, liquid-crystal displays, touch screen displays, etc.[3,4] In addition, graphene modified with heteroatoms is known to exhibit catalytic activity for oxygen reduction reaction, which can be available for the cathode in fuel cells.[5,6] Although the applications to various kinds of devices are expected, the effect of UV-light on the device performance is not fully understood. To date, several studies have reported that UV-irradiation causes the carrier doping to graphene.[7−11] Luo et al. and Yurgens et al. reported *n*-type doping,[7,8] wheras Iqbal et al. found *p*-type doping by UV-irradiation.[9] This difference might be ascribed to the experimental conditions under which UV-irradiation was performed. As the adsorbates are likely to decompose via photochemical reaction, the difference in environment would provide different kinds of doping to graphene. To obtain a comprehensive understanding about the effect of UV-irradiation on the transport properties of graphene, the experiment under well-controlled conditions is required.

Here we report the effect of UV-irradiation on the electrical properties of graphene on SiO_2. The graphene/SiO_2 field effect transistor (FET) was exposed to UV-irradiation in a vacuum ($\sim 10^{-6}$ Pa), and the change of FET characteristics was pursued in situ. UV-irradiation decreased the mobility and gave rise to a hysteresis in the transfer characteristics. Subsequent annealing in a vacuum eliminated the hysteresis but caused *n*-type doping. On the basis of the transport measurements and Raman spectroscopy, we discuss the phenomenological model for the UV-irradiation to graphene on SiO_2.

EXPERIMENTAL SECTION

A monolayer graphene purchased from Graphene Laboratories Inc. was used in this study. Figure 1 shows a schematic illustration of the experimental setup with the FET structure on SiO_2 (285 nm)/Si. Gold electrodes (20 nm) deposited on the monolayer graphene were used as the source/drain electrodes. After the source, drain, and gate electrodes were wired through the electrical feedthroughs, the chamber was evacuated to $\sim 10^{-6}$ Pa, in which UV-irradiation and FET measurements were performed. At first, the samples were annealed in a vacuum at 160 °C for several hours to remove the surface contaminants and adsorbates. This annealing moved the charge neutrality point (CNP) to 0 V, whereas the CNP of the as-received sample was located at >80 V due to the *p*-type doping by adsorbed water and oxygen.[12,13] We employed a deuterium lamp (L2D2, 30 W, Hamamatsu Photonics K.K.) as a UV-light source. The UV spectrum exhibits a maximum between 150 and 200 nm, and the effective power on the graphene surface was estimated at ~ 0.01 mW/cm^2. Raman spectroscopy with an excited wavelength of 532 nm (JASCO NRS-3100) was used to characterize the graphene. The Raman measurements were performed under atmospheric conditions.

Received: October 16, 2014
Accepted: January 8, 2015
Published: January 8, 2015

 © 2015 American Chemical Society

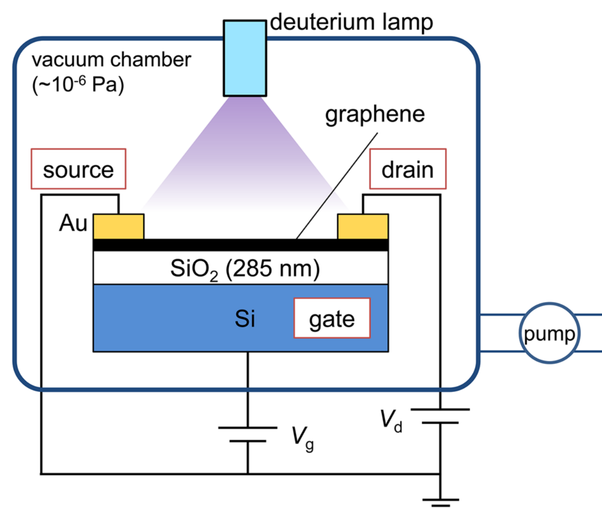

Figure 1. Schematic illustration of graphene FET.

RESULTS AND DISCUSSION

According to the procedure described above, the graphene/SiO_2 FET was UV-irradiated in a vacuum for 5 h. Figure 2a shows the change of FET characteristics at various stages. Before the UV-irradiation, the device exhibits typical transfer characteristics of graphene FET with a CNP at around 0 V. The mobility (μ) is 1800 $cm^2/(V\ s)$ for electron transport, and 2400 $cm^2/(V\ s)$ for hole transport. After the UV-irradiation, two noticeable features can be seen from Figure 2a: evolution of a hysteresis and the decrease of mobility. The hysteresis in the transfer characteristics is counterclockwise on the negative side and clockwise on the positive side. Electron mobility (μ_e) and hole mobility (μ_h) for the forward sweep (negative to positive gate voltage) decreased to 640 and 760 $cm^2/(V\ s)$, respectively. (μ_e and μ_h for the backward sweep are 800 and 700 $cm^2/(V\ s)$, respectively.) The reduction in mobility implies the defect formation in graphene.[14] The device was then annealed in a vacuum at 160 °C for 3 h. After the annealing, the mobility partially recovers; μ_e and μ_h are 1800 and 1300 $cm^2/(V\ s)$, respectively. Simultaneously, the hysteresis behavior disappears and the CNP shifts to the negative direction. In addition, we performed repeated cycles of the UV-irradiation and the annealing on the graphene sample on a SiO_2/Si substrate. It has been observed that the hysteresis behavior appears after each UV-irradiation process (Figure S1a in the Supporting Information). The shift in the CNP levels off at a negative value after the cycles (Figure S1b in the Supporting Information).

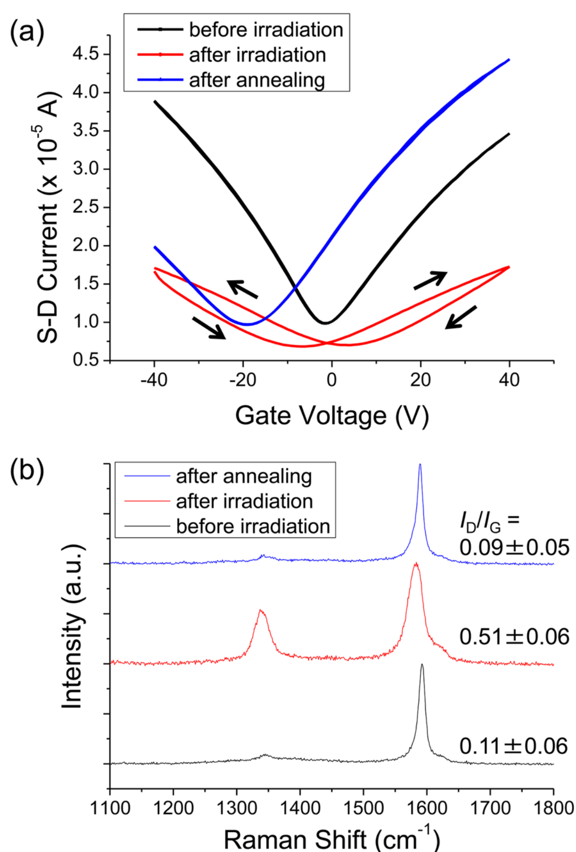

Figure 2. (a)Transfer characteristics of graphene UV-irradiated in a vacuum. (b) Raman spectra of graphene UV-irradiated in a vacuum. Note that the spectra labeled "before irradiation" and "after annealing" are obtained from the same device in panel a. The spectrum labeled "after irradiation" is from another graphene FET sample after UV-irradiation.

Figure 2b shows the change of Raman spectrum by the UV-irradiation and the subsequent annealing. All the spectra exhibit the G band at ~1580 cm^{-1}, arising from E_{2g} vibrational mode of sp^2 carbon network. The sharp and symmetric 2D band appears at 2687.0 ± 1.6 cm^{-1}, which indicates the graphene is monolayer (Figure S2a in Supporting Information).[15] A small peak at ~1350 cm^{-1} can be seen for the sample before irradiation. This peak is the D band, which corresponds to the A_{1g} vibrational mode of sp^2 carbon hexagons. As the D band becomes Raman active when the sp^2 carbon network has defects such as vacancies and disorders, the intensity ratio of the D band to the G band (I_D/I_G) is used as a good indicator to evaluate the density of defects.[16] A small I_D/I_G for the graphene before irradiation (I_D/I_G = 0.11 ± 0.06) means that the graphene initially contains few defects. An evolution of the D band after the UV-irradiation indicates the increase of defect density. Therefore, the decrease of carrier mobility observed in the FET measurement is considered to relate closely with the induced defects. Raman I_D/I_G mapping on the UV-irradiated sample shows that defects were uniformly formed in the channel region (Figure S3 in the Supporting Information). The subsequent annealing at 160 °C decreases I_D/I_G to 0.09 ± 0.05, which is equivalent to that of the graphene before the UV-irradiation. Thus, the defects induced by UV-irradiation in a vacuum are fully recovered by annealing at 160 °C. In addition, the G band red-shifts after the UV-irradiation: from 1592.7 ± 1.8 cm^{-1} to 1586.1 ± 1.8 cm^{-1}. In contrast, the 2D band is not shifted by UV-irradiation or subsequent annealing: 2684 ± 4 and 2686 ± 3 cm^{-1} for "after irradiation" and "after annealing", respectively (Figure S2a in the Supporting Information).

Figure 3a shows the time dependence of the I_D/I_G. The I_D/I_G increases monotonically with increasing irradiation time to 5 h. On the other hand, the difference between the two charge neutrality points of a transfer characteristics (ΔV) levels off in less than 1 h, as shown in Figure 3b. The different dependence on the irradiation time indicates that defect formation and emergence of the hysteresis behavior are not coincidental phenomena.

To consider the origin of the UV-induced defects, Ar^+ bombardment to graphene was performed for comparison. The sample was bombarded with Ar^+ with an acceleration

DOI: 10.1021/am5071464
ACS Appl. Mater. Interfaces 2015, 7, 2439−2443

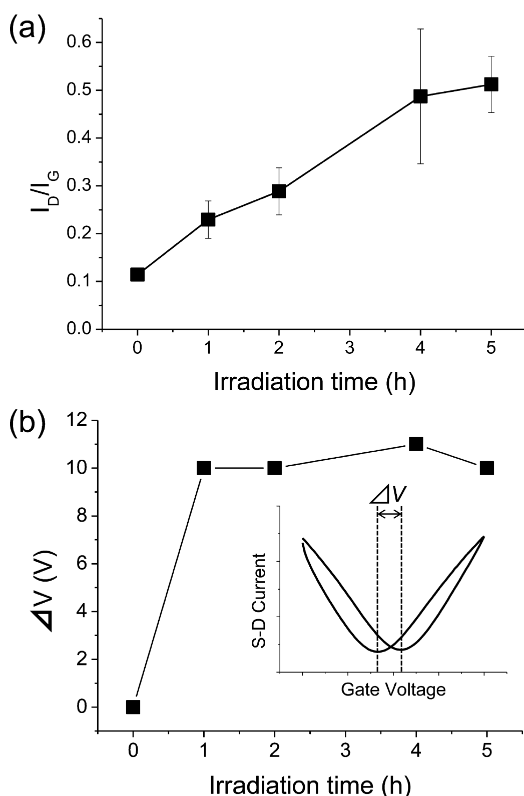

Figure 3. Irradiation-time dependence of (a) I_D/I_G and (b) ΔV for UV-irradiated samples.

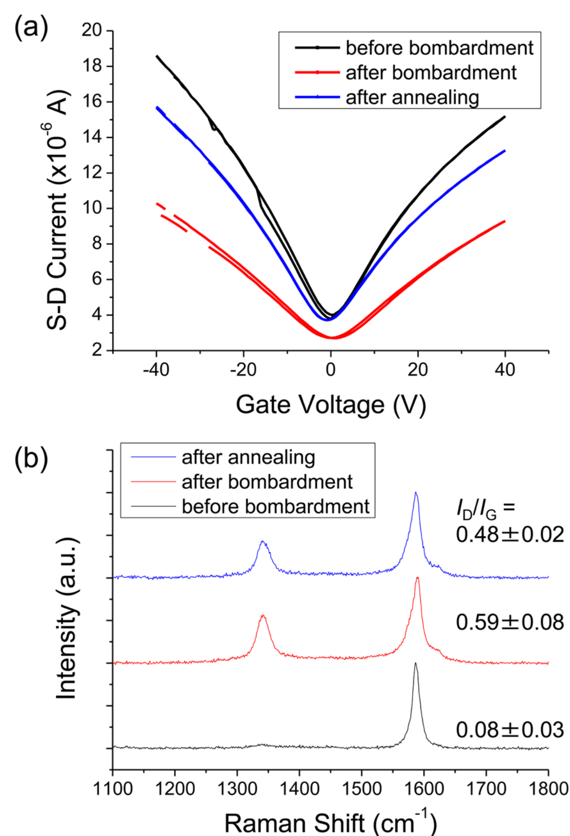

Figure 4. (a)Transfer characteristics of Ar^+ bombarded graphene. (b) Raman spectra of Ar^+ bombarded graphene. Note that the spectra labeled "before bombardment" and "after annealing" are obtained from the same device in (a). The spectrum labeled "after bombardment" is from another graphene FET sample after UV-irradiation.

voltage of 300 eV. The Ar pressure was fixed at 1.0×10^{-3} Pa, and the bombardment duration was set at 7 s so as to make I_D/I_G similar to that of the UV-irradiated graphene in Figure 2b. In the case of Ar^+ bombardment, part of the carbon atoms are sputtered and thus the possible defects are structural vacancies.[17] Figure 4a shows the FET characteristics at the various stages: before and after Ar^+ bombardment, and after subsequent annealing at 160 °C. The mobility decreases with Ar^+ bombardment; μ_e and μ_h decrease to 1100 and 1200 from 2300 and 2500 cm^2/(V s), respectively. In contrast to the UV-irradiation, a hysteresis behavior is not observed. As in the case of UV-irradiation, annealing the sample in a vacuum at 160 °C for 3 h partially recovers the mobility. (μ_e and μ_h are 1800 and 2200 cm^2/(V s), respectively) However, the CNP is not shifted by Ar^+ bombardment and subsequent annealing.

Figure 4b shows the Raman spectral change accompanying with the Ar^+ bombardment and subsequent annealing. Compared to the UV-irradiation, I_D/I_G ratio only slightly decreases (0.59 ± 0.03 to 0.48 ± 0.02) after the annealing. It has been reported that vacancy defects are partially repaired by annealing at low temperatures (~200 °C).[17,18] The displaced carbon atoms and/or the PMMA residue might partially recover the vacancies at 160 °C. This partial restoration is consistent with the FET measurement where the mobility recovers by annealing. The red-shift of the G band observed in the UV-irradiated graphene is not seen for the Ar^+ bombarded graphene (1590 ± 2 cm^{-1} and 1588.1 ± 1.9 cm^{-1} for before and after Ar^+ bombardment, respectively). No noticeable changes were observed for the 2D band (Figure S2b in the Supporting Information).

On the basis of the experimental results, we discuss the defect formation mechanism by UV-irradiation in a vacuum. The decrease of the mobility and the increase of I_D/I_G indicate that defects were formed by UV-irradiation in a vacuum. This kind of defect was, however, restored by annealing at as low as 160 °C, whereas the defects induced by Ar^+ bombardment, mostly structural vacancies, were not fully recovered by annealing at such a low temperature.[17,18] A structural disorder like Stone−Wales (SW) defects nor explains the UV-induced defects because the energy necessary to restore a SW defect (4.0 eV) is much larger than the thermal energy of annealing at 160 °C.[19]

With regard to the possible defects induced by UV-irradiation in a vacuum, we assume that sp^3-like bonds are formed by UV-irradiation. (Figure 5) It has been known that a SiO_2 surface has silanol groups and adsorbed water molecules even after annealing at 160 °C.[20,21] De Rosa et al. reported that UV-irradiation to SiO_2 in water gives rise to the increase of −OH groups at the surface.[22] Although the detailed mechanism for the reaction is still unknown, their experimental result indicates the photodissociation of O−H bonds of water molecules. In the present experiment, O−H bonds of adsorbed water and/or silanol groups can be photodissociated by UV-irradiation, resulting in the formation of hydrogen radicals (H·), hydroxyl radicals (·OH) and Si−O·. In addition, Si−O bonds are homolytically broken to the radicals (−Si·, −Si−O·).[23] These radicals tend to react with the graphene lattice and cause sp^3-like bonds in the graphene lattice. In the absorption spectrum of graphene, a peak appears at 4.6 eV (270 nm) that corresponds to π-band saddle point (M point) transition.[24]

DOI: 10.1021/am5071464
ACS Appl. Mater. Interfaces 2015, 7, 2439−2443

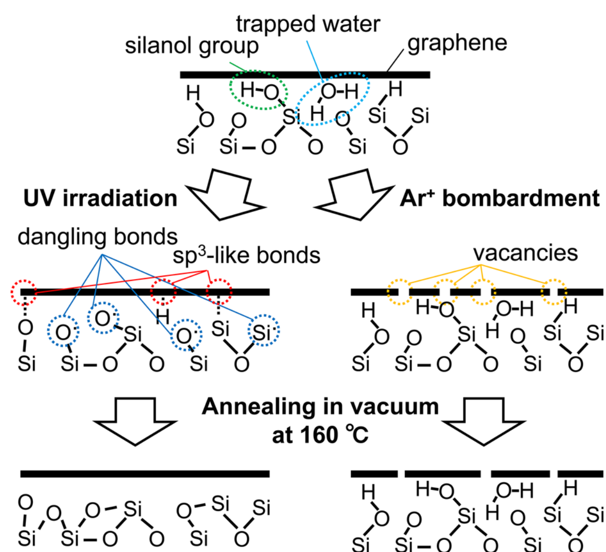

Figure 5. Schematic illustration of defect formation by UV irradiation and Ar^+ bombardment.

Such an electronic transition may enhance a chemical reaction between graphene and radicals or dangling bonds at the SiO_2 surface. Moreover, it is known that the graphene on SiO_2 has inherent corrugations, which enhance the reactivity of graphene.[25−27] Therefore, such virtual sp^3-like bonds are likely to be formed locally at the points, where the distance between the graphene and SiO_2 is closer. The red-shift of the G band (Figure 2b) also supports this model. As Ryu et al. have reported that hydrogenation of graphene red-shifts the G band as a result of charge doping,[28] it is reasonable that the formation of such chemical bonds gives rise to the red-shift of the G band by UV-irradiation.

The formation of sp^3-like bonds by photoirradiation was also reported by Kanasaki et al.[29] They observed sp^3-bonded carbon nanoscale domains on a highly oriented pyrolytic graphite (HOPG) surface by femtosecond-laser excitation. Although the photon energy and flux are different from our study, sp^2 carbon atoms in graphene/graphite can be converted to sp^3-like carbon by photoirradiation.

The radicals caused by UV-irradiation act likely as the dangling bonds on the SiO_2 surface. Because the dangling bonds are known to trap carriers in the channel of the FET device, the formation of such dangling bonds is responsible for the hysteresis behavior.[30,31] Charge injection between the graphene and the interface can explain the observed hysteresis behavior in the transfer characteristics: counterclockwise on the negative side and clockwise on the positive side.[32] When the V_g is negative with respect to the CNP, holes are injected from graphene to the interface state. The charge density of the injected holes ΔQ_s causes the shift of CNP by $-e\Delta Q_s/C_{ox} < 0$ when V_g sweeps from negative to CNP, resulting in counterclockwise hysteresis on the negative side. (e and C_{ox} are the elementary charge and the capacitance of SiO_2 per area, respectively.) The absence of hysteresis after Ar^+ bombardment also supports the above discussion because the vacancy defects do not create carrier traps like dangling bonds (Figure 5). Therefore, it is inferred that dangling bonds are created at the SiO_2 surface by UV-irradiation, which trap carriers and yield the hysteresis in the transfer characteristics. Since hysteresis appears by UV-irradiation after the annealing (Figure S1a in the Supporting Information), dangling bonds caused by the breakage of Si−O bonds can be mainly responsible for the carrier traps. The trapped carriers can also contribute to the decreased mobility because the trapped carriers at graphene/SiO_2 interface cause remote Coulomb scattering.[33]

As we have seen in Figure 3, formation of defects (sp^3-like bonds) and creation of carrier traps (dangling bonds) are not coincidental phenomena. To discuss more quantitatively, we estimate the density of sp^3-like bonds (n_d) and the density of trapped carriers (n_c) from the Raman I_D/I_G and ΔV in the transfer characteristic, respectively. According to the Tuinstra−Koenig relation, the crystalline size (L_D), an average distance between defects, is written as $L_D = C/(I_D/I_G)$, where C is a constant depending on the excitation wavelength.[34,35] As n_d is described as $n_d = 1/L_D^2$, n_d can be written as $n_d = (I_D/I_G)^2/C^2$. In the case of UV-irradiation for 5 h (Figure 3), n_d is estimated to 6.8×10^{10} cm^{-2}. From the relationship for a capacitor, n_c can be written as $n_c = C_{ox}\Delta V_{CNP}/e$, where ΔV_{CNP} is the shift in the charge neutrality point. When $\Delta V_{CNP} = \Delta V/2 = 5$ V, as in the case of UV-irradiation for 5 h (Figure 3), n_c is estimated to $n_c = 4.1 \times 10^{11}$ cm^{-2}, which is higher than n_d by 1 order of magnitude.

Considering that I_D/I_G and ΔV show different dependence on the irradiation time, and the density of n_c is much higher than that of n_d, we discuss the phenomenological model for the formation of sp^3-like defects and dangling bonds. By UV-irradiation to graphene on SiO_2, dangling bonds are formed at a SiO_2 surface and the density of the dangling bonds levels off in less than 1 h. In contrast to the fast process for the formation of dangling bonds, the formation of sp^3-like bonds is much slower. Because the I_D/I_G does not increase even if the sample is left in a vacuum for a longer time after the UV-irradiation, graphene cannot react with the dangling bonds spontaneously. A monotonic increase of I_D/I_G with irradiation time (Figure 3b) implies that formation of sp^3-like bonds requires UV-light. Thus, UV-irradiation triggers the reaction between graphene and the SiO_2 surface (or the dangling bonds), which proceeds much slower than the formation of dangling bonds.

The sp^3-like bonds are possibly broken by annealing at 160 °C.[28] The annealing also eliminate the dangling bonds, resulting in the disappearance of the hysteresis behavior. The shift of CNP to the negative direction after annealing is caused by electron doping from the clean SiO_2 surface, which Romero et al. has found both experimentally and theoretically.[36] In the present work, the silanol groups and adsorbed water molecules existing on the pristine SiO_2 surface were converted to other chemical species that can be decomposed at 160 °C. These species were eliminated by the annealing at 160 °C, and the graphene comes to contact more directly with the clean SiO_2 surface resulting in the n-type doping.

■ CONCLUSION

In conclusion, we studied the effect of UV-irradiation on the FET characteristics of graphene on SiO_2/Si under a well-controlled condition, and proposed a phenomenological model. UV-irradiation gives rise to the formation of dangling bonds and sp^3-like bonds at the graphene/SiO_2 interface, which cause the hysteresis and the decreased mobility. The subsequent annealing breaks the sp^3-like bonds and removes the dangling bonds, leading to recovery of the mobility and disappearance of the hysteresis. UV-irradiation and annealing realizes the intrinsic graphene/SiO_2 interface, at which electron doping occurs from the SiO_2 surface to graphene. The present experimental results show that the graphene/SiO_2 interface is

DOI: 10.1021/am5071464
ACS Appl. Mater. Interfaces 2015, 7, 2439−2443

crucial for the instability of graphene to UV-light, and will give a clue to enhance the durability of graphene based devices.

■ ASSOCIATED CONTENT

Supporting Information

Cycles of UV-irradiation and annealing, Raman spectra including the 2D band region, and Raman I_D/I_G mapping image of the UV-irradiated sample. This material is available free of charge via the Internet at http://pubs.acs.org.

■ AUTHOR INFORMATION

Corresponding Author

*G. Imamura. Tel/Fax: +81-4-7136-3904. E-mail: imamura@epi.k.u-tokyo.ac.jp.

Notes

The authors declare no competing financial interest.

■ ACKNOWLEDGMENTS

This work was partially supported by the New Energy and Industrial Technology Development Organization (NEDO).

■ REFERENCES

(1) Novoselov, K. S.; Fal'ko, V. I.; Colombo, L.; Gellert, P. R.; Schwab, M. G.; Kim, K. A Roadmap for Graphene. *Nature* **2012**, *490*, 192−200.

(2) Choi, H.; Jung, S.; Seo, J.; Chang, D. W.; Dai, L.; Baek, J. Graphene for Energy Conversion and Storage in Fuel Cells and Supercapacitors. *Nano Energy* **2012**, *1*, 534−551.

(3) Yin, Z.; Zhu, J.; He, Q.; Cao, X.; Tan, C.; Chen, H.; Yan, Q.; Zhang, H. Graphene-based Materials for Solar Cell Applications. *Adv. Energy Mater.* **2014**, *4*, 1300574.

(4) Huang, X.; Zeng, Z.; Fan, Z.; Liu, J.; Zhang, H. Graphene-based Electrodes. *Adv. Mater.* **2012**, *24*, 5979−6004.

(5) Huang, S.; Terakura, K.; Ozaki, T.; Ikeda, T.; Boero, M.; Oshima, M.; Ozaki, J.; Miyata, S. First-Principles Calculation of the Electronic Properties of Graphene Clusters Doped with Nitrogen and Boron: Analysis of Catalytic Activity for the Oxygen Reduction Reaction. *Phys. Rev. B* **2009**, *80*, 235410.

(6) Yang, Z.; Nie, H.; Chen, X.; Chen, X.; Huang, S. Recent Progress in Doped Carbon Nanomaterials as Effective Cathode Catalysts for Fuel Cell Oxygen Reduction Reaction. *J. Power Sources* **2013**, *236*, 238−249.

(7) Luo, Z.; Pinto, N. J.; Davila, Y.; Johnson, A. T. C. Controlled Doping of Graphene Using Ultraviolet Irradiation. *Appl. Phys. Lett.* **2012**, *100*, 253108.

(8) Yurgens, A.; Lindvalla, N.; Suna, J.; Nama, Y.; Park, Y. W. Control of the Dirac Point in Graphene by UV Light. *JETP Lett.* **2013**, *98*, 704−708.

(9) Iqbal, M. Z.; Siddique, S.; Iqbal, M. W.; Eom, J. Formation of p−n Junction with Stable p-Doping in Graphene Field Effect Transistors Using Deep UV irradiation. *J. Mater. Chem. C* **2013**, *1*, 3078−3083.

(10) Mitoma, N.; Nouchi, R. Gate-Controlled Ultraviolet Photo-Etching of Graphene Edges. *Appl. Phys. Lett.* **2013**, *103*, 201605.

(11) Meng, J.; Wu, H.; Chen, J.; Lin, F.; Bie, Y.; Shvets, I. V.; Yu, D.; Liao, Z. Ultraviolet Irradiation-Controlled Memory Effect in Graphene Field-Effect Transistors. *Small* **2013**, *9*, 2240−2244.

(12) Joshi, P.; Romero, H. E.; Neal, A. T.; Toutam, V. K.; Tadigadapa, S. A. Intrinsic Doping and Gate Hysteresis in Graphene Field Effect Devices Fabricated on SiO_2 Substrates. *J. Phys.: Condens. Matter* **2010**, *22*, 334214.

(13) Ryu, S.; Liu, L.; Berciaud, S.; Yu, Y.; Liu, H.; Kim, P.; Flynn, G. W.; Brus, L. E. Atmospheric Oxygen Binding and Hole Doping in Deformed Graphene on a SiO_2 Substrate. *Nano Lett.* **2010**, *10*, 4944−4951.

(14) Chen, J.; Cullen, W. G.; Jang, C.; Fuhrer, M. S.; Williams, E. D. Defect Scattering in Graphene. *Phys. Rev. Lett.* **2009**, *102*, 236805.

(15) Ferrari, A. C.; Meyer, J. C.; Scardaci, V.; Casiraghi, C.; Lazzeri, M.; Mauri, F.; Piscanec, S.; Jiang, D.; Novoselov, K. S.; Roth, S.; Geim, A. K. Raman Spectrum of Graphene and Graphene Layers. *Phys. Rev. Lett.* **2006**, *97*, 187401.

(16) Malard, L. M.; Pimenta, M. A.; Dresselhaus, G.; Dresselhaus, M. S. Raman Spectroscopy in Graphene. *Phys. Rep.* **2009**, *473*, 51−87.

(17) An, B.; Fukuyama, S.; Yokogawa, K.; Yoshimura, M. Evolution of Ar^+-Damaged Graphite Surface during Annealing As Investigated by Scanning Probe Microscopy. *J. Appl. Phys.* **2002**, *92*, 2317−2322.

(18) Chen, J.; Shi, T.; Cai, T.; Xu, T.; Sun, L.; Wu, X.; Yu, D. Self Healing of Defected Graphene. *Appl. Phys. Lett.* **2013**, *102*, 103107.

(19) Meng, L.; Jiang, J.; Wang, J.; Ding, F. Mechanism of Metal Catalyzed Healing of Large Structural Defects in Graphene. *J. Phys. Chem. C* **2014**, *118*, 720−724.

(20) Chua, L.; Zaumseil, J.; Chang, J.; Ou, E. C.; Ho, P. K.; Sirringhaus, H.; Friend, R. H. General Observation of n-Type Field-Effect Behaviour in Organic Semiconductors. *Nature* **2005**, *434*, 194−199.

(21) Zhuravlev, L. T. The Surface Chemistry of Amorphous Silica. Zhuravlev Model. *Colloids Surf., A* **2000**, *173*, 1−38.

(22) DeRosa, R. L.; Schader, P. A.; Shelby, J. E. Hydrophilic Nature of Silicate Glass Surfaces as a Function of Exposure Condition. *J. Non-Cryst. Solids* **2003**, *331*, 32−40.

(23) Kajihara, K.; Ikuta, Y.; Oto, M.; Hirano, M.; Skuja, L.; Hosono, H. UV−VUV Laser Induced Phenomena in SiO_2 Glass. *Nucl. Instrum. Methods Phys. Res., Sect. B* **2004**, *218*, 323−331.

(24) Mak, K. F.; Shan, J.; Heinz, T. F. Seeing Many-Body Effects in Single- and Few-Layer Graphene: Observation of Two-Dimensional Saddle-Point Excitons. *Phys. Rev. Lett.* **2011**, *106*, 046401.

(25) Meyer, J. C.; Geim, A. K.; Katsnelson, M. I.; Novoselov, K. S.; Booth, T. J.; Roth, S. The Structure of Suspended Graphene Sheets. *Nature* **2007**, *446*, 60−63.

(26) Boukhvalov, D. W.; Katsnelson, M. I. Enhancement of Chemical Activity in Corrugated Graphene. *J. Phys. Chem. C* **2009**, *113*, 14176−14178.

(27) Imamura, G.; Saiki, K. Interlayer Interaction in the UV Irradiated Defect Formation of Graphene. *J. Phys. Chem. C* **2014**, *118*, 11842−11848.

(28) Ryu, S.; Han, M. Y.; Maultzsch, J.; Heinz, T. F.; Kim, P.; Steigerwald, M. L.; Brus, L. E. Reversible Basal Plane Hydrogenation of Graphene. *Nano Lett.* **2008**, *8*, 4597−4602.

(29) Kanasaki, J.; Inami, E.; Tanimura, K.; Ohnishi, H.; Nasu, K. Formation of sp3-Bonded Carbon Nanostructures by Femtosecond Laser Excitation of Graphite. *Phys. Rev. Lett.* **2009**, *102*, 087402.

(30) Roh, Y.; Kim, K.; Jung, D. The Hysteresis Caused by Interface Trap and Anomalous Positive Charge in $Al/CeO_2-SiO_2/Silicon$ Capacitors. *Jpn. J. Appl. Phys.* **1997**, *36*, 1681−1684.

(31) Sekine, K.; Saito, Y.; Hirayama, M.; Ohmi, T. Silicon Nitride Film Growth for Advanced Gate Dielectric at Low Temperature Employing High-Density and Low-Energy Ion Bombardment. *J. Vac. Sci. Technol. A* **1999**, *17*, 3129−3133.

(32) Liu, Z.; Bol, A. A.; Haensch, W. Large-Scale Graphene Transistors with Enhanced Performance and Reliability Based on Interface Engineering by Phenylsilane Self-Assembled Monolayers. *Nano Lett.* **2011**, *11*, 523−528.

(33) Li, M.-Y.; Tang, C.-C.; Ling, D. C.; Li, L. J.; Chi, C. C.; Chen, J.-C. Charged Impurity-Induced Scatterings in Chemical Vapor Deposited Graphene. *J. Appl. Phys.* **2013**, *114*, 233703.

(34) Tuinstra, F.; Koenig, J. L. Raman Spectrum of Graphite. *J. Chem. Phys.* **1970**, *53*, 1126−1130.

(35) Lucchese, M. M.; Stavale, F.; Martins Ferreira, E. H.; Vilani, C.; Moutinho, M. V. O.; Capaz, R. B.; Achete, C. A.; Jorio, A. Quantifying Ion-Induced Defects and Raman Relaxation Length in Graphene. *Carbon* **2010**, *48*, 1592−1597.

(36) Romero, H. E.; Shen, N.; Joshi, P.; Gutierrez, H. R.; Tadigadapa, S. A.; Sofo, J. O.; Eklund, P. C. n-Type Behavior of Graphene Supported on Si/SiO_2 Substrates. *ACS Nano* **2008**, *2*, 2037−2044.

DOI: 10.1021/am5071464
ACS Appl. Mater. Interfaces 2015, 7, 2439−2443